A SEMI-ANALYTIC, MATRIX-BASED MODEL FOR THE BEAM ARRIVAL TIME JITTER

M.A. Johnson*[1,2], P.H. Williams[1,2]
[1]ASTeC, STFC Daresbury Laboratory, Sci-Tech Daresbury, Warrington WA4 4AD, UK
[2]The Cockcroft Institute, Sci-Tech Daresbury, Warrington, WA4 4AD, UK

Abstract

The beam arrival time jitter is an important parameter for many advanced electron accelerators, including next-generation XFEL drivers. Accurate jitter modelling is particularly important during the design of a new facility, where it is often used to determine the tolerances of the RF sources and photoinjector laser. Conventionally, jitter is modeled using computationally intensive start-to-end simulations; in this approach, the entire accelerator is simulated many times, while the parameter associated with each jitter source is varied within its expected tolerance. This approach is time-consuming and scales poorly with the size and complexity of the accelerator. Semi-analytic jitter models therefore have significant advantages, owing to their speed and greater insight into the underlying physics. In this contribution, we propose a simple matrix-based model for the arrival time jitter in a linear accelerator with an arbitrary layout. We validate the model against simulations of CLARA at Daresbury Laboratory, and use it to explore the jitter tolerances of different operating modes.

INTRODUCTION

Many advanced electron accelerators require tight control of the beam arrival time to achieve their maximum performance. For instance, plasma wakefield acceleration (PWFA) schemes using external injection typically require synchronization of the electron beam to within a few femtoseconds, to keep the beam energy jitter within tolerable limits [1,2]. Likewise, next-generation X-ray free electron laser (XFEL) concepts are likely to place stringent limits on the synchronization of the electron beam, potentially requiring sub-femtosecond timing jitter.

In recent years, several accelerator facilities have targeted state-of-the-art synchronization using a variety of schemes. For example, SwissFEL [3] has achieved an RMS arrival time jitter (ATJ) of ~10 fs by optimizing the performance of their RF systems to meet demanding stability requirements [4]. The ARES linac at DESY [5] aims to generate extremely short (sub-fs) electron bunches with an ATJ of $\lesssim 10$ fs using a variety of bunch compression schemes [6,7].

Understanding how the ATJ develops along an accelerator is particularly important during the design of a new facility. Accurate jitter modelling can provide insights into how different design choices will affect the stability requirements of the accelerator subsystems, including the RF sources and photoinjector laser. For example, accelerators that use arcs for bunch compression may benefit from a reduced ATJ due to the so-called ‘magic angle’ effect [8,9].

Detailed studies of the ATJ often rely on start-to-end accelerator simulations, which can require significant computational resources [10,11]. Conventionally, the ATJ is evaluated by considering an ensemble of simulations, where the parameter representing each jitter source has been randomly varied within its expected tolerance. While this approach is straightforward, it is often time-consuming and quickly becomes impractical for larger, more complex accelerators.

Considerable insight into the ATJ can be obtained using simple semi-analytic models, which can be orders of magnitude faster while offering a deeper understanding of the underlying physics. These models can quickly estimate the ATJ for different accelerator operating points, making them useful during both the design and operation of a facility. In recent years, several models have been proposed for the ATJ in linear electron accelerators [12–15]. However, these models are often only valid for a specific accelerator layout, or a particular type of bunch compression scheme.

In this paper, we propose a semi-analytic jitter model that is valid for any linear electron accelerator with an arbitrary layout. The model is derived by considering the joint statistical distribution of the beam’s arrival time jitter and energy jitter. Lattice elements that affect the beam’s jitter distribution are represented as matrix transformations, providing a simple way to propagate different jitter sources along an accelerator. Our model combines physics insights from a number of recent studies [8,9,15] and defines a single, self-consistent framework for estimating the ATJ.

SEMI-ANALYTIC MODEL

Photoinjector

The coupled equations for the longitudinal dynamics in a standing wave RF cavity can be written as [15,16]

$$\frac{\mathrm{d}\gamma}{\mathrm{d}z} = 2\alpha k\, \varepsilon_z(z) \cos(\phi + kz) \tag{1}$$

and

$$\frac{\mathrm{d}\phi}{\mathrm{d}z} = k\left(\frac{\gamma}{\sqrt{\gamma^2 - 1}} - 1\right), \tag{2}$$

where γ is the Lorentz factor of the beam, k is the RF wavenumber, and z denotes longitudinal distance along the axis of the cavity. The function $\varepsilon_z(z) \approx \cos(kz)$ is the dimensionless, normalized field profile of the cavity. The parameter $\alpha = qE_0/2kmc^2$ is the normalized RF gradient, where E_0 is the peak electric field inside the cavity, and q

---

* mark.johnson@stfc.ac.uk

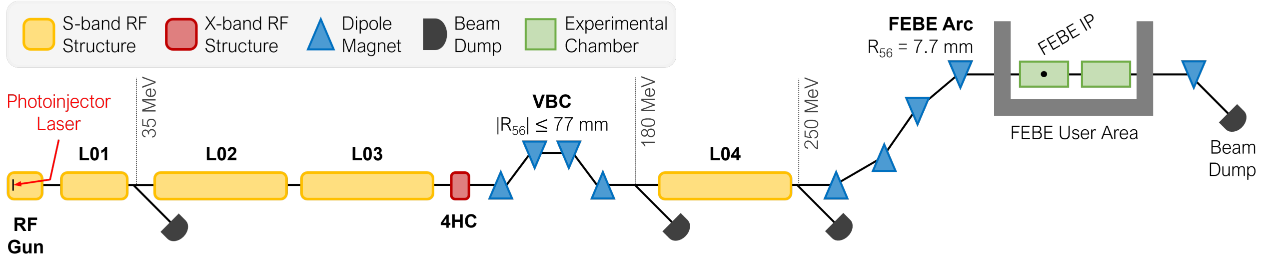

Figure 1: Simplified schematic of the CLARA linear accelerator at STFC Daresbury Laboratory. Components that are not relevant to this study are not shown for clarity.

and m are the charge and rest mass of the electron respectively. We define $\phi = \phi_i + \omega t - kz$ as the RF phase seen by the electron bunch as it traverses the cavity, where ϕ_i is the initial RF phase, ω is the RF angular frequency, and t is the time elapsed since the beam first entered the cavity.

In an RF photoinjector, electron bunches are generated when a pulsed laser strikes a cathode at the back plane of an RF cavity. If the laser pulse arrives later than expected, the electrons will leave the cathode surface t_{las} later than an ideal ‘reference bunch’ with no jitter. The initial RF phase seen by the beam is therefore $\phi_i = \phi_0 + \omega t_{\text{las}}$, where ϕ_0 is the initial phase experienced by the reference bunch.

Integrating Equations 1 and 2 gives the Lorentz factor γ_f and RF phase ϕ_f of an electron bunch at the exit of the gun. Small changes in the laser timing and RF parameters will induce variation in the properties of the outgoing beam; to first order, we can write that [15]

$$\begin{pmatrix} \mathrm{d}t \\ \mathrm{d}E \end{pmatrix} = \begin{pmatrix} \partial t/\partial \alpha & \partial t/\partial \phi_0 & \partial t/\partial t_{\text{las}} \\ \partial E/\partial \alpha & \partial E/\partial \phi_0 & \partial E/\partial t_{\text{las}} \end{pmatrix} \begin{pmatrix} \mathrm{d}\alpha \\ \mathrm{d}\phi_0 \\ \mathrm{d}t_{\text{las}} \end{pmatrix}, \tag{3}$$

where $\mathrm{d}E \simeq mc^2 \mathrm{d}\gamma_f$ represents a small change in the final beam energy, and $\mathrm{d}t$ is a small change in the beam arrival time relative to the reference bunch. The arrival time can be written in terms of the final RF phase as

$$\mathrm{d}t = \frac{1}{\omega}\left(\mathrm{d}\phi_f - \mathrm{d}\phi_0\right) . \tag{4}$$

The Jitter Covariance Matrix

As shown by Eq. (3), shot-to-shot fluctuations in the photoinjector RF and laser parameters will lead to variation in the outgoing beam properties. To represent the joint statistical distribution of the beam’s arrival time jitter and energy jitter, we introduce the jitter covariance matrix

$$\Sigma_{\text{beam}} = \begin{pmatrix} \langle \mathrm{d}t^2 \rangle & \langle \mathrm{d}t\,\mathrm{d}E \rangle \\ \langle \mathrm{d}t\,\mathrm{d}E \rangle & \langle \mathrm{d}E^2 \rangle \end{pmatrix} . \tag{5}$$

The jitter covariance matrix is evaluated by considering the properties of many electron bunches passing through a specific point along the accelerator lattice. From Eq. (4), the jitter covariance immediately after an RF photoinjector can be written as

$$\Sigma_{\text{gun}} = \mathbf{J}_{\text{gun}} \begin{pmatrix} \langle \mathrm{d}\alpha^2 \rangle & \langle \mathrm{d}\alpha\,\mathrm{d}\phi_0 \rangle & 0 \\ \langle \mathrm{d}\alpha\,\mathrm{d}\phi_0 \rangle & \langle \mathrm{d}\phi_0^2 \rangle & 0 \\ 0 & 0 & \langle \mathrm{d}t^2 \rangle \end{pmatrix} \mathbf{J}_{\text{gun}}^T , \tag{6}$$

where $\mathbf{J}_{\text{gun}}$ is the Jacobian matrix defined in Eq. (3). The matrix written in expanded form is the covariance of the gun RF and laser parameters; the laser timing is assumed to be independent of the RF phase and gradient.

Accelerating Cavities

Having derived an expression for the jitter covariance immediately after an RF photoinjector, we now derive how the jitter distribution evolves as the beam passes through various lattice elements. For an ultra-relativistic beam with negligible phase slippage, the average beam energy after an RF accelerating cavity can be written as

$$E_f = E_i + qV_{\text{RF}} \cos\left(\phi + n\omega t_i\right) \tag{7}$$

where V_{RF} and ϕ are the nominal RF voltage and off-crest phase, respectively, for a cavity operated at the n^{th} harmonic of the accelerator’s primary RF frequency. E_i are E_f are the input and output beam energies, respectively, while t_i denotes the arrival time of the incoming electron bunch relative to the reference bunch.

By taking derivatives of Eq. (7), we can approximate how the final beam energy will depend on different jitter sources as [12]

$$\begin{pmatrix} \mathrm{d}t_f \\ \mathrm{d}E_f \end{pmatrix} = \mathbf{A} \begin{pmatrix} \mathrm{d}t_i \\ \mathrm{d}E_i \end{pmatrix} + \mathbf{B} \begin{pmatrix} \mathrm{d}\phi \\ \mathrm{d}\tilde{V} \end{pmatrix} , \tag{8}$$

with

$$\mathbf{A} = \begin{pmatrix} 1 & 0 \\ -nq\omega V_{\text{RF}} \sin\phi & 1 \end{pmatrix} \tag{9}$$

and

$$\mathbf{B} = qV_{\text{RF}} \begin{pmatrix} 0 & 0 \\ -\sin\phi & \cos\phi \end{pmatrix} . \tag{10}$$

where $\mathrm{d}\tilde{V} = \mathrm{d}V/V_{\text{RF}}$. Based on Eq. (8), the jitter covariance matrix will transform as

$$\Sigma_{\text{beam},\,f} = \mathbf{A}\Sigma_{\text{beam},\,i}\mathbf{A}^T + \mathbf{B}\Sigma_{\text{RF}}\mathbf{B}^T , \tag{11}$$

where Σ_{RF} is the covariance matrix of the RF phase and relative voltage, respectively. Writing Eq. (11) in terms of an RF covariance matrix allows us to account for klystron-induced correlations between the RF phase and voltage [17]. These correlations can be exploited to achieve a reduced ATJ at specific accelerator operating points [8, 9].

Table 1: RMS beam energy jitter and beam arrival time jitter at various points along CLARA (Fig. 1) for a standard operating mode. For comparison, we include estimates from both the semi-analytic model and start-to-end simulations.

Location	**Beam Energy [MeV]**	**Arrival Time Jitter [fs]**		**Energy Jitter [%]**	
		Simulation	Semi-analytic	Simulation	Semi-analytic
Post-L01	35	150 ± 10	155.0	0.08 ± 0.01	0.09
Post-VBC	180	98 ± 6	108.6	0.15 ± 0.01	0.17
FEBE IP	250	65 ± 4	81.2	0.11 ± 0.01	0.13

Bunch Compressors

In many accelerators, one or more bunch compressors are used to manipulate the electron bunch length. The arrival time jitter of an electron bunch immediately after a bunch compressor can be written as

$$\mathrm{d}t_f = \mathrm{d}t_i + \frac{R_{56}}{c}\frac{\mathrm{d}E_i}{E}\,, \tag{12}$$

where R_{56} is the first-order longitudinal dispersion of the bunch compressor, and c is the speed of light in vacuum. The jitter covariance matrix will therefore transform according to Eq. (8), with $\mathbf{B} = 0$ and

$$\mathbf{A} = \begin{pmatrix} 1 & R_{56}/cE \\ 0 & 1 \end{pmatrix}. \tag{13}$$

MODEL VALIDATION

To validate the semi-analytic model, we applied it to a typical linear accelerator with multiple RF cavities and bunch compression stages. CLARA (Fig. 1) is a high-brightness electron beam facility at STFC Daresbury Laboratory [18, 19]. The accelerator is comprised of a high-repetition-rate (400 Hz) electron gun [20] followed by four S-band accelerating structures. A chicane-type variable bunch compressor (VBC) is located between the third and fourth linacs, along with an X-band linearizer for longitudinal phase space correction [21]. A 16-meter-long arc connects CLARA to the full energy beam exploitation (FEBE) area, a separately-shielded enclosure where the majority of user experiments take place [22].

For this study, we implemented the semi-analytic model as `python` library, which includes a numerical representation for each type of lattice element. As described elsewhere, there is no simple analytical solution for the equation of motion in an RF photoinjector (Eq. (1) and (2)). Following the approach in [15], we solve the equations of motion numerically, and calculate the associated Jacobian matrix (Eq. (3)) via automatic differentiation using PyTorch [23].

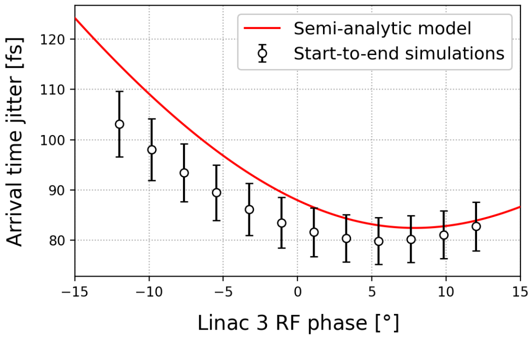

Figure 2: Calculation of the RMS arrival time jitter after the final linac (see Fig. 1) as a function of the Linac 3 RF phase.

To validate our model, we compare it against jitter estimates obtained from start-to-end CLARA simulations using ASTRA [24] and ELEGANT [25]. A detailed description of these simulation methods can be found elsewhere [10, 11]. We assume a photoinjector laser timing jitter of 200 fs, an RF phase jitter of 0.1 °, and an RF amplitude jitter of 5×10^{-4}.

Table 1 and Fig. 2 compare jitter calculations with the semi-analytic model against equivalent estimates from start-to-end simulations. The model is typically accurate to within $\lesssim$10 fs; any differences are likely due to collective effects, particularly in the RF gun, which are not included in the semi-analytic model. Whereas jitter estimates using start-to-end simulations typically take several hours on a desktop PC, the semi-analytic model provides an estimate in a few seconds. Figure 3 demonstrates how the model can be used to explore how the ATJ depends on different machine parameters.

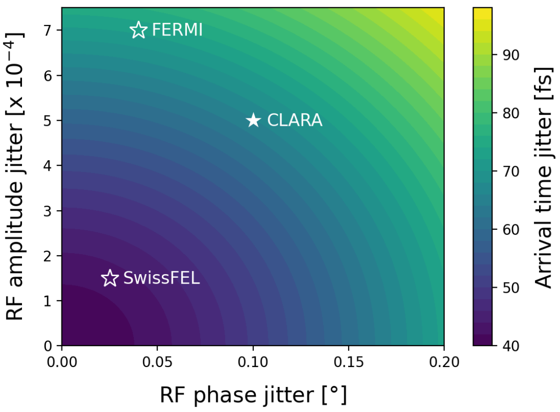

Figure 3: ATJ at the FEBE IP (see Fig. 1) as a function of RF phase and amplitude jitter. The solid marker indicates the assumed RF tolerances for CLARA. The hollow markers indicate the expected performance of the CLARA layout if it had the reported RF stability of other named facilities [4,26].

CONCLUSIONS

In this contribution, we have briefly outlined a simple model for the beam arrival time jitter, which can be applied to linear electron accelerators with a variety of layouts. In future, we plan to validate the model against experimental measurements on CLARA, and benchmark it against other accelerator facilities with a broad range of beam parameters.

REFERENCES

[1] J. Grebenyuk, R.W. Assmann, U. Dorda and B. Marchetti, "Laser-driven Acceleration with External Injection at SINBAD", *in Proc. IPAC'14*, Dresden, Germany, Jun. 2014, pp. 1515-1518. `doi:10.18429/JACoW-IPAC2014-TUPME064`

[2] C.A. Lindstrøm, "Staging of Plasma-wakefield Accelerators", *Phys. Rev. Accel. Beams* **24**, 014801, 2021. `doi:10.1103/PhysRevAccelBeams.24.014801`

[3] E. Prat, R. Abela, M. Aiba *et al.*, "A Compact and Cost-effective Hard X-ray Free-electron Laser Driven by a High-brightness and Low-energy Electron Beam", *Nature Photonics* **14**, 748-754, 2020. `doi:10.1038/s41566-020-00712-8`

[4] C. Beard *et al.*, "RF System Performance in the SwissFEL Linac", *in Proc. LINAC'22*, Liverpool, UK, Aug.-Sep. 2022, pp. 679-684 `doi:10.18429/JACoW-LINAC2022-TH2AA02`

[5] J. Zhu, R. Assmann, U. Dorda and B. Marchetti, "Lattice Design and Start-to-end Simulations for the ARES Linac", *Nucl. Instrum. Methods Phys. Res. Sect. A* **909**, 467, 2018

[6] J. Zhu, R.W. Assmann, M. Dohlus, U. Dorda and B. Marchetti, "Sub-fs Electron Bunch Generation with Sub-10-fs Bunch Arrival-time Jitter via Bunch Slicing in a Magnetic Chicane" *Phys. Rev. Accel. Beams* **19**, 054401, 2016 `doi:10.1103/PhysRevAccelBeams.19.054401`

[7] T. Vinatier *et al.*, "Characterization of Relativistic Electron Bunch Duration and Traveling Wave Structure Phase Velocity Based on Momentum Spectra Measurements", *Phys. Rev. Accel. Beams* **27**, 022801, 2024. `doi:10.1103/PhysRevAccelBeams.27.022801`

[8] E. Mansten, R. Svärd, S. Thorin, M. Eriksson and P. Fernandes Tavares, "Cancellation of Klystron-induced Energy and Arrival-time Variations in Linear Accelerators with Arc-type Bunch Compressors", *Phys. Rev. Accel. Beams* **27**, 040401, 2024. `doi:10.1103/PhysRevAccelBeams.27.040401`

[9] A. Dixon, P. Williams, S. Thorin, T. Charles and A. Wolski, "Reduction of Arrival Time Jitter or Energy Spread with Arclike Variable Bunch Compressors", *Phys. Rev. Accel. Beams* **27**, 110702, 2024. `doi:10.1103/PhysRevAccelBeams.27.110702`

[10] B.P.M. Liggins, J.W. McKenzie, P.H. Williams, and J.K. Jones, "Jitter Tolerance for CLARA", *in Proc. IPAC'13*, Shanghai, China, May 2013, pp. 1271-1273.

[11] M. Johnson, J. Jones and P. Williams, "Jitter Tolerance for the FEBE Beamline on CLARA", *in Proc. IPAC'23*, Venice, Italy, May 2023, pp. 2071-2074. `doi:10.18429/JACoW-IPAC2023-TUPL143`

[12] P. Craievich, S. Di Mitri, M. Milloch, G. Penco and F. Rossi, "Modeling and Experimental Study to Identify Arrival-time Jitter Sources in the Presence of a Magnetic Chicane", *Phys. Rev. ST Accel. Beams* **16**, 090401, 2013. `doi:10.1103/PhysRevSTAB.16.090401`

[13] R. Pompili *et al.*, "Femtosecond Timing-jitter Between Photocathode Laser and Ultra-short Electron Bunches by Means of Hybrid Compression", *New J. Phys.* **18**, 083033. `doi:10.1088/1367-2630/18/8/083033`

[14] A. Vorozhtsov *et al.*, "The Soft X-ray Laser at MAX IV - Conceptual Design Report", pp. 65-75, 2021. `http://www.maxiv.lu.se/soft-x-ray-laser/`

[15] T. Xu, F. Ji, C.J.R. Duncan, S.P. Weathersby and R.J. England, "Calculation of RF-induced Temporal Jitter in Ultrafast Electron Diffraction", *Phys. Rev. Accel. Beams* **28**, 024001, 2025. `doi:10.1103/PhysRevAccelBeams.28.024001`

[16] K.J. Kim, "RF and Space-charge Effects in Laser-driven RF Electron Guns", *Nucl. Instrum. Methods Phys. Res. Sect. A* **275**, 201, 1989 `doi:10.1016/0168-9002(89)90688-8`

[17] Y. Liu, H. Matsumoto, L. Li *et al.*, "Analysis the Influence of Pulse-to-pulse Stability of Modulator on High-power Microwave Output of Pulsed Klystron", *SN Appl. Sci.* **4**, 4, 2022 `doi:10.1007/s42452-021-04889-7`

[18] J.A. Clarke, D. Angal-Kalinin, N. Bliss, R. Buckley *et al.*, "CLARA Conceptual Design Report", *J. Instrum.* **9** T05001, 2014. `doi:10.1088/1748-0221/9/05/T05001`

[19] D. Angal-Kalinin, M.A. Johnson, J.K. Jones, T.H. Pacey *et al.*, "CLARA Commissioning and First Friendly User Experiments", presented at IPAC'26, Deauville, France, May 2026, this conference.

[20] J.W. McKenzie, L.S. Cowie, P. Goudket, B.L. Militsyn *et al.*, "High Repetition Rate S-band Photoinjector Design for the CLARA FEL", *in Proc. FEL'14*, Basel, Switzerland, Aug. 2014, pp. 889-892.

[21] L.S. Cowie, A.D. Brynes, J.K. Jones *et al.*, "An X-Band Lineariser for the CLARA FEL", *in Proc. IPAC'18*, Vancouver, Canada, Apr. - May 2018, pp. 3848-3851. `doi:10.18429/JACoW-IPAC2018-THPAL084`

[22] E.W. Snedden, D. Angal-Kalinin, A.R. Bainbridge *et al.*, "Specification and Design for Full Energy Beam Exploitation of the Compact Linear Accelerator for Research and Applications", *Phys. Rev. Accel. Beams* **27**, 041602, 2024. `doi:10.1103/PhysRevAccelBeams.27.041602`

[23] A. Paszke, S. Gross, F. Massa *et al.*, "PyTorch: An Imperative Style, High performance Deep Learning Library", in *Advances in Neural Information Processing Systems* 32, 2019, pp. 8024-8035 `doi:10.48550/arXiv.1912.01703`

[24] K. Flöttmann, ASTRA, `https://www.desy.de/~mpyflo/`

[25] M. Borland, "Elegant: A Flexible SDDS-Compliant Code for Accelerator Simulation", Advanced Photon Source LS-287, September 2000.

[26] S. Di Mitri, private communication, Apr. 2026.